Some statistical inferences of parameter in MCMC approach and the application in uncertainty analysis of hydrological simulation

Pengfei Shi[a,b,c], Tao Yang[a,b,c*], Bin Yong[a,c], Chong-Yu Xu[d], Zhenya Li[a], Xiaoyan Wang[a], Youwei Qin[a], Xudong Zhou[a]

a State Key Laboratory of Hydrology-Water Resources and Hydraulic Engineering, Center for Global Change and Water Cycle, Hohai University, Nanjing 210098, China;

b Yangtze Institute for Conservation and Development, Hohai University, Jiangsu, 210098, China;

c College of Hydrology and Water Resources, Hohai University, Nanjing 210098, China;

d Department of Geosciences, University of Oslo, P.O. Box 1047, Blindern, 0316 Oslo, Norway;

Key points:

- Parameter σ^2 in MCMC approach is interpreted and estimated through statistical inference and theoretical analysis
- A new label called Confidence Level of Model (*CLM*) is developed to guide the

---

*Corresponding author:
Dr. Tao Yang, Professor
State Key Laboratory of Hydrology-Water Resources and Hydraulic Engineering
Center for Global Change and Water Cycle
Hohai University, Nanjing 210098
The People's Republic of China
Tel: (+86) 25 83786017
E-mail: tao.yang@hhu.edu.cn

estimation of parameter σ^2

- The natural logarithm of the posterior probability distribution for Nash-Sutcliffe Coefficient of Efficiency (*NSCE*) is a first-order linear equation associated with *CLM*
- The MCMC method based on *CLM* performs well in generating regular posterior distributions of model parameters and discharges, and in yielding narrow and symmetrical confidence intervals

Abstract: Markov Chain Monte Carlo (MCMC) method has been increasingly popular in uncertainty analysis of hydrological simulation. In MCMC approach, deviations between model outputs and observations are commonly assumed to follow Gaussian distribution with zero medium and constant standard deviation σ^2. However, the estimation of σ^2 is a difficulty in terms of that it was assigned subjectively in previous studies, hindering the improvement of performance for uncertainty assessment. This work systemically investigates the statistical meaning of parameter σ^2. σ could be expressed as the product of data length and two standard deviations, one of which is for observations (i.e. σ_{Obs}) and the other for Nash-Sutcliffe Coefficient of Efficiency (*NSCE*) (i.e. σ_s). A new label called Confidence Level of Model (*CLM*) is developed to interpret σ_s. The natural logarithm of the posterior probability distribution for *NSCE* is a first-order linear equation associated with *CLM*. The *CLM* could be employed to guide the construction of σ_s and then the estimation of σ^2. Uncertainty analysis of a flow duration curve (FDC) model is conducted using the MCMC method based on *CLM*, and the generalized likelihood uncertainty estimation (GLUE) method is employed for comparison. Results show that the *CLM* affects the MCMC results by three kinds of trade-offs, and the MCMC method based on *CLM* performs well in generating regular

posterior distributions of model parameters and discharges. The MCMC method also yields narrow and symmetrical confidence intervals. Findings of this paper could interpret typical uncertainty behaviors commonly existing in hydrological modeling, and provide beneficial insights for the uncertainty analysis of other environmental modeling.

Keywords: Uncertainty analysis; Markov Chain Monte Carlo (MCMC) method; parameter; hydrological simulation; Flow duration curve (FDC) model.

1. Introduction

A number of statistical methods have been proposed to quantify the uncertainty of hydrological simulation (Ren et al., 2018), for examples, the Taylor expansion-based methods (Naji et al., 1998), the stochastic response surface (SRS) method (Cryer and Applequist, 2003) and the Rosenblueth's method (Rosenblueth, 1975). Nonetheless, most approaches suffer from the typical difficulties commonly encountered in classical statistic inferences, such as the determination of statistics for hypothesis testing and prior probability distribution for model outputs. These difficulties are even severely deteriorated for a model whose parameter space features discontinuous derivate, multimodality and curing multidimensional ridges (Vrugt et al., 2003a). Thus, an advanced uncertainty analysis method is urgently needed for assessing the uncertainty of hydrological simulation.

The Bayesian approaches have been increasingly popular in uncertainty analysis of models including some complex distributed models (Kuczera et al., 2010; Marshall et al., 2004, 2005; Thiemann et al., 2001; Ajami et al., 2007). Bayesian inference is theoretically more reasonable, computationally much simpler, and is demonstrated superior to classical statistics in many studies (Kuczera and Parent, 1998; Vrugt et al, 2009). It meanwhile provides the posterior distributions of model parameters and outputs (Bouda et al., 2011; Kavetski et al., 2006). Bayesian approaches provide a beneficial means to evaluate the uncertainty of hydrological models or simulation.

Bayesian approaches could be classified into two classes: the pseudo-Bayesian (or informal) method and standard (or formal) Bayesian method. The Generalized Likelihood Uncertainty Estimate (GLUE) methodology (Beven and Binley, 1992) is the most widely-used pseudo-Bayesian method (Beven and Freer, 2001; Hassan et al., 2008; Choi and Beven, 2007) whose target posterior distributions are commonly selected to be statistically informal distributions (Vrugt et al., 2009). Practical experiments show that the accuracy of GLUE method relies on the choice of likelihood functions and cut-off threshold to a great degree, especially for complex high-dimension cases (Kuczera et al., 2007; Blasone et al., 2008a). The sampling direction and step is not well controlled and adjusted, likely leading to poor sampling and convergence efficiency. The Markov Chain Monte Carlo (MCMC) method is a typical standard Bayesian approach (Kuczera and Parent, 1998; Reis et al, 2005). In the case of hydrological simulation, MCMC method assumes that the residuals between model outputs and observations follow independent identically distributed (i.i.d.) distribution (Jin et al., 2010; Chung and Kim, 2013). The directional sampling strategy of MCMC (e.g. Metropolis-Hasting sampling, Gibbs sampling) promises the convergence of samples to target posterior distribution (Kuczera and Parent, 1998). Nevertheless, poor choices of prior distribution, proposal distribution and parameters in MCMC may lead to unsatisfying convergence efficiency (Engeland and Gottschalk, 2002). A lot of studies were carried out to increase the convergence efficiency (Ouarda et al., 2011; Lee and Kim, 2008; Huang et al., 2018; Li et al., 2018a), and a number of revised

MCMC approaches were developed, for instance, the Shuffled Complex Evolution Metropolis (SCEM-UA) method (Vrugt et al., 2003a, 2003b), Sequence Evolution Metropolis (EMC) method (Zhang et al., 2009) and Bayesian Total Error Analysis (BATEA) approach (Kavetski et al., 2006).

The pre-establishment of algorithmic parameters is vital to obtain the target posterior distribution in the above MCMC approaches. Efforts have been devoted to studying the algorithmic parameters. The i.i.d. distribution of residuals is normally assumed to be Gaussian distribution with zero medium and constant variance σ^2 (Yang et al., 2007; Bouda et al., 2011; Ajami et al., 2007; Li et al., 2018b; Li et al., 2018c). Thiemann et al (2001) suggested a σ^2 ranging from 25% to 50% of the variance of the long-term discharges. It is however ambiguous to treat parameter σ^2 as constant. Some researchers removed σ^2 by assuming a non-informative prior density $p(\theta,\sigma_t \mid \beta) \propto \sigma^{-1}$ (Vrugt et al., 2003a). Other reports treated σ^2 as one of the unknown model parameters that needed to be sampled (Liang et al., 2005; Zhang et al., 2009). Limited studies try to interpret the statistical meaning of parameter σ^2, hindering the improvement of MCMC approaches. Consequently, a proper interpretation and estimation of σ^2 in the case of Gaussian-type i.i.d. distribution is of urgent needed.

This work aims to: (1) build a new label called Confidence Level of Model (*CLM*) to interpret and estimate the parameter σ^2, (2) present uncertainty analysis of hydrological simulation using MCMC approach, and (3) reveal the effect of *CLM* on the results of uncertainty analysis.

2. Methodology

2.1 Bayesian approaches for uncertainty analysis

Given input-output series (x, y), model $M(\cdot)$ and parameter set θ, model outputs then could be expressed as follows:

$$\tilde{y} = M(x, \theta) \tag{1}$$

Bayesian statistics treats model parameters as probabilistic variables and aims at obtaining the real parameter distribution by incorporating prior information with the sample information. A prior probability density $\pi(\theta)$ is used to reflect analysts' knowledge about model parameters. A likelihood function implies the sample information. Bayesian inference is formulated as follows:

$$\pi(\theta \mid x, y, \tilde{y}) = \frac{f(\tilde{y} \mid \theta, x, y)\pi(\theta)}{\int f(\tilde{y} \mid \theta, x, y)\pi(\theta)d\theta} \tag{2}$$

Where, $\pi(\theta \mid x, y, \tilde{y})$ is the posterior probability of parameter set θ conditioned by input-output series (x, y); $f(\tilde{y} \mid \theta, x, y)$ denotes the likelihood function, which is commonly written in another form $l(\theta \mid x, y, \tilde{y})$.

$$\pi(\theta \mid x, y, \tilde{y}) = \frac{l(\theta \mid x, y, \tilde{y})\pi(\theta)}{\int l(\theta \mid x, y, \tilde{y})\pi(\theta)d\theta} \tag{3}$$

Or

$$\pi(\theta \mid x, y, \tilde{y}) \propto l(\theta \mid x, y, \tilde{y})\pi(\theta) \tag{4}$$

The prior distribution is assumed a non-informative distribution. The likelihood function thus significantly affects the results of Bayesian inference.

2.1.1 Markov Chain Monte Carlo (MCMC) algorithm

The residuals between observations and model outputs are expressed as

$$e_i = y_i - \tilde{y}_i = y_i - M(x_i, \theta) \qquad i = 1, 2, \cdots, n \tag{5}$$

Consider the residuals to be Gaussian-type i.i.d. distribution with zero medium and constant variance $\sigma_t^{\,2}$

$$p(e_i \mid \theta) = \frac{1}{\sqrt{2\pi}\sigma_t} \exp\left(-\frac{e_i^2}{2\sigma_t^{\,2}}\right) \tag{6}$$

If the residuals do not follow Gaussian distribution, Box-Cox transformation is applied before the Metropolis-Hasting judgment (Thyer et al., 2002)

$$z = \begin{cases} (y^{\lambda} - 1)/\lambda & \lambda \neq 0 \\ In(y) & \lambda = 0 \end{cases} \tag{7}$$

The likelihood function $l(\theta \mid x)$ is the multiple product of probabilities for all residuals (Vrugt et al., 2003a; Zhang et al., 2009)

$$l(\theta \mid x) = \prod_{i=1}^{n} \frac{1}{\sqrt{2\pi\sigma_t}} \exp(-\frac{e_i^2}{2\sigma_t^{\,2}}) = (2\pi)^{-n/2} \sigma_t^{\,-n} \exp(-\frac{\sum_{i=1}^{n} e_i^{\,2}}{2\sigma_t^{\,2}}) \tag{8}$$

Providing a uniform prior and removing the constant term, the posterior probability could be established.

$$p(\theta \mid x) = l(\theta \mid x)\pi(\theta) \propto \exp(-\frac{\sum_{i=1}^{n} e_i^{\,2}}{2\sigma_t^{\,2}}) \tag{9}$$

Eq.8 is the formal likelihood measure derived from robust statistical philosophy, reflecting the statistical nature of residuals. The general MCMC sampling is given as below (Vrugt et al., 2003b).

Step 1: Randomly select a start point θ_i in the feasible parameter space, and calculate the posterior probability $p(\theta_i \mid x)$.

Step 2: Generate a new candidate point θ_{i+1} according to a proposal distribution $z(\theta_{i+1} \mid \theta_i)$, and calculate the posterior probability $p(\theta_{i+1} \mid x)$ of θ_{i+1}.

Step 3: Metropolis-Hasting judgment: (1) randomly sample a label Z over the interval [0, 1]; (2) compute $\Omega = \min\{1, p(\theta_{i+1} \mid x) / p(\theta \mid x)\}$; (3) if $Z < \Omega$, accept the candidate point θ_{i+1}, otherwise retain at the current position, $\theta_{i+1} = \theta_i$.

Step 4: Increments *t*. If *t* is less than the pre-identified population size *N*, return to step 1.

In this work, we focus on the algorithmic parameter σ_t in Eq.8, which is an important parameter but always treated ambiguously in previous studies.

2.2 Interpretation of the algorithmic parameter

The posterior probability (Eq.9) could be adapted as

$$p(\theta \mid x) \propto \exp(-\frac{\sum_{i=1}^{n} e_i^2}{2\sigma_t^2}) = \exp[-\frac{\sum_{i=1}^{n}(Sim_i - Obs_i)^2 \cdot \sum_{i=1}^{n}(Obs_i - \overline{Obs})^2}{2\sigma_t{}^2 \sum_{i=1}^{n}(Obs_i - \overline{Obs})^2}] \tag{10}$$

The unbiased estimation of the standard deviation for observations is formulated as

$$\sigma_{obs} = \sqrt{\frac{1}{n-1}\sum_{i=1}^{n}(Obs_i - \overline{Obs})^2} \tag{11}$$

Integrating Eq.11 and the equation of Nash-Sutcliffe Coefficient of Efficiency (*NSCE*) (Eq. 27) into Eq.10 obtains

$$p(\theta \mid x) \propto \exp[-\frac{(n-1)\sigma_{obs}{}^2}{2\sigma_t{}^2}\frac{\sum_{i=1}^{n}(Sim_i - Obs_i)^2}{\sum_{i=1}^{n}(Obs_i - \overline{Obs})^2}] = \exp[-\frac{1\text{- NSCE}}{2(\frac{\sigma_t}{\sqrt{n-1}\sigma_{obs}})^2}] \tag{12}$$

$$= \exp(-\frac{s^2}{2\sigma_s{}^2})$$

Where

$$s = \sqrt{1 - NSCE} \tag{13}$$

$$\sigma_t = \sqrt{n-1}\sigma_{Obs};\sigma_s \tag{14}$$

The original posterior probability is turned into normal distribution with the introduction of new variable *s* and σ_s. As a variable associated with *NSCE*, *s* could be regarded as the measure for the distance from the present model state to the ideal model state (i.e. *NSCE*=1, *s*=0).The algorithmic parameter σ_t is expressed as the product of data length ($\sqrt{n-1}$) and two standard deviations (σ_{Obs} and σ_s). Therefore, it could be concluded that σ_t is statistically related not only to the observation but also to model calibration.

2.2.1 Posterior probability of *s* and *NSCE*

Eq.12 is the formula for posterior probability of parameter set θ rather than variable *s*. Supposing that the sample population is generated by a MCMC approach (Figure 1(a)), it is possible that an *s* corresponds to a number of samples (e.g. the samples in area Ω_{S1} and Ω_{S2}). If we put all samples with the same *s* (i.e. same $NSCE_c$) into an interval Ω_S (*S*=1, 2, 3, … n), the posterior probability of variable *s* could be written as

$$p(s|x) = \int_{\Omega_S} p(\theta|x)d\theta \propto Area(s)\exp\left(-\frac{s^2}{2\sigma_s^2}\right) \tag{15}$$

Where, $Area(s)$ is the ratio of the Ω_S space to the whole sample population space and $\int_0^{+\infty} Area(s)ds = 1$, $\exp\left(-\frac{s^2}{2\sigma_s^2}\right)$ is the right half of a normal distribution (shown in Figure.1(c)). If we expect *P*% of the total MCMC samples to yield acceptable model outputs, there is $\sigma_s = \hat{s}/[2\varphi^{-1}(P\%)]$, where $\hat{s}$ denotes maximum *s* of acceptable sample and $\phi^{-1}(\cdot)$ is the inverse function of standard normal probability density. The *NSCE* corresponding to $\hat{s}$ (Eq. 13), named Confidence Level of Model (*CLM*) in this paper, is expressed as

$$CLM = 1 - 4[\sigma_s \cdot \varphi^{-1}(P\%)]^2 \tag{16}$$

Then we can obtain

$$\sigma_t = \sqrt{(n-1)(1-CLM)} \cdot \sigma_{obs} / [2\varphi^{-1}(P\%)]^2 \tag{17}$$

To remove $Area(s)$ from Eq. 15, assume the prior distribution of $Area(s)$ as a uniform prior density:

$$Area(s) \propto 1 \tag{18}$$

Hence we can get

$$p(s \mid x) \propto \exp\left[-\frac{2\varphi^{-2}(P\%)s^2}{1-CLM}\right] \tag{19}$$

The posterior probability distribution of parameter θ (Eq. 12) is transformed to that of *s* (Eq. 19). As to *NSCE*, an *s* corresponds to only one *NSCE*, indicating that $p(s \mid x) = p(NSCE \mid x)$. Here we take the natural logarithm of the posterior probability for *NSCE* with *P*% set as 95%:

$$In(p(NSCE \mid x)) = \frac{5.4NSCE}{1-CLM} - \left\{ In\left[\sqrt{\pi(1-CLM)}/1.64\right] + \frac{5.4}{1-CLM} \right\} \tag{20}$$

Eq. 20 is a first-order linear equation of *NSCE* with an intercept of $-\left\{ In\left[\sqrt{\pi(1-CLM)}/1.64\right] + \frac{5.4}{1-CLM} \right\}$ at the horizontal axis as well as a slope of $\frac{5.4NSCE}{1-CLM}$. Eq. 19 and 20 are demonstrated by practical experiment in the section 4.2.3 later.

2.2.2 Interpretation of *CLM*

CLM could be interpreted as the manually-decided minimum acceptable *NSCE* according to the inferences above. It seems that *CLM* in MCMC method plays a similar role as the cut-off threshold (shorten as CT) used in GLUE method. Actually, these two labels are significantly different. Firstly, *CLM* is a procedure-oriented label that has the function of controlling the shape of target distribution. Whereas, CT is a result-oriented label acting on the already-generated sample population, which aims at removing the non-behavioral samples with *NSCE* lower than CT. In short, *CLM* acts as outlet of a funnel and CT acts as a sieve (Figure. 1(b)). The parameter space out of *CLM* could still be searched with small probabilities, whereas this part is entirely cut off by CT. Besides, *CLM* can be deemed as a probabilistic variable or a constant, which is however impossible for CT.

2.2.3 *CLM* acting as a constant or a probabilistic variable

σ_t is commonly assumed to be a constant or a probabilistic variable referring to the handlings in previous studies.

(1) If σ_t is a constant, the *CLM* is

$$CLM = 1 - 4[\sigma_t \cdot \varphi^{-1}(P\%) / \sigma_{obs}]^2 / (n-1) \tag{21}$$

Given a common setting $\sigma_t = k \cdot \sigma_{obs}$ ($0 < k \le 1$) and *P*%=95%, Eq. 21 can be expressed as

$$CLM = 1 - 10.82k^2 / (n-1) \tag{22}$$

Apparently, *CLM* approaches to 1 with the extension of time series.

(2) If σ_t is a probabilistic variable with density $f(\sigma_t)$, it is inferred as

$$F(\sigma_{ct}) = P(\sigma_t < \sigma_{ct}) = P(CLM > CLM_c) = 1 - F(CLM_c) - P(CLM_c) \tag{23}$$

Where, σ_{ct} is a variance corresponding to a certain constant, and CLM_c is a CLM value corresponding to σ_{ct}.

The probability density $g(CLM)$ is therefore expressed as

$$\begin{aligned} g(CLM) &= \frac{d(1 - F(\sigma_t) - P(CLM_c))}{dCLM} = -\frac{dF(\sigma_t)}{d\sigma_t} \cdot \frac{d\sigma_t}{dCLM} \\ &= \frac{\sqrt{n-1}\sigma_{obs}}{4\sqrt{1-CLM}\,\varphi^{-1}(P)} \cdot f(\sqrt{(n-1)(1-CLM_c)} \cdot \sigma_{obs} / \varphi^{-1}(P\%))) \\ &\propto \frac{1}{\sqrt{1-CLM}} \cdot f(\sigma_t(CLM)) \end{aligned} \tag{24}$$

Consequently, the probabilistic property of σ_t from experts' knowledge is interpreted by the changes of *CLM*. Providing a Jeffrey prior $p(\sigma) \propto \sigma^{-1}$(a common setting), the corresponding prior of *CLM* could be obtained

$$g(CLM) \propto \frac{1}{1-CLM} \qquad CLM < 1 \tag{25}$$

The prior *CLM* evidently follows a similar distribution with the Jeffrey σ_t prior.

Algorithmic parameter σ_t is abstract whereas the concept of *CLM* is concrete. It is hence readily to identify the prior information of *CLM* rather than that of algorithm parameter σ_t.

2.2.4 Influence of *CLM* on sampling results

It is seen in Figure 1(c), the right part of normal distribution is the target posterior distribution. All samples just fall into the right side of *s*, which could be identified as the meaningful section. Figure 1(d) shows the percentage of the meaningful section to target distribution versus the change of *CLM* provided that the best fitting *NSCE* of a hydrological model in a watershed is 0.9. It could be observed that the percentage decrease slightly in low *CLM* section whereas sharply in middle and high *CLM* section. A very small ratio likely fails to generate sample population in consistence with target posterior distribution. A relatively small *CLM* (corresponding to high percentage) is therefore recommended to tackle this issue. On the other hand, the slope of probability density at *s* (*NSCE*=0.9) is shown in Figure 1(d). A proper slope ensures a promising occupation of the high probability space and a sufficient occupation over the low probability space. Too high slope makes heavily clustered sample population lack of sample diversity, while too low slope loses the ability of locating at the high probability space and results in frequent exchange of samples between the low and high probability spaces. The slope peaks at *CLM*=0.9 and extremely declines when *CLM* approaches to 1. Details concerning the influence of *CLM* to the sampling results will be presented in section 4.

3. Study area and Hydrological simulation

3.1 Study area and data

The Huangheyan region (20,930 km^2), at an altitude of 4200 to 4800 m a.s.l, is located at the head of the Yellow river. The region shows a typical continental climate with hot summer and dry winter since it is far away from oceans (Cui et al., 2018; Shi et al., 2017; Kumar et al., 2019). Lack of human activities makes it an ideal natural hydrological system. The mean annual precipitation ranges from 200 to 400mm, more than 70% of which falls intensively from July to October, and 62% of the whole precipitation is snowfall. The mean annual temperature is ranged between -4℃ and 2℃ (Wang et al., 2018) and the mean annual evapotranspiration is about 1322mm (denoted by 20mm evaporating pan) (Wang et al., 2017). The data involved in this study is the observed daily discharge records at outlet of Huangheyan region during the period 1996-2000. The data are collected from the local hydrology bureau and the National Climate Center.

Besides, five basins including Dongwan, Luanchuan, Tantou, Xiquan and Zijingguan, are employed to further demonstrate the *CLM* method (Eq. 16-20). Dongwan, Luanchuan and Tantou are located in Yellow River basin, Xiquan belongs to Liao River basin, and Zijingguan is a part of Hai River Basin. These three large rivers play the key role in sustaining the social and economy development of North China.

3.2 Four-parameter flow duration curve (FDC) model

Flow duration curve (FDC) model can describe the statistical relationship between the *i*th discharge in descending order and the probabilities it is exceeded (Shao et al., 2009; Yang et al., 2017). It is hence widely accepted as an informative method for displaying the complete range of river discharges from low flows to flood events (Guse et al., 2016). FDCs commonly take on various shapes according to the climatic and geomorphic characteristics in the area of interest. In this work, a four-parameter FDC model proposed by Shao (2009) is employed for simulating the discharge.

$$q(p;\alpha,\beta,\overline{Q},\tau,\theta)=\begin{cases}\dfrac{\overline{Q}(-\beta)^{\alpha+1}}{B(\alpha+1,-\alpha-\beta^{-1})}\left[\left\{1-(p/\tau)^{\beta}\right\}/\beta\right]^{\alpha}(1-p/\tau)^{\theta} & \beta<0\\ \dfrac{\tau\overline{Q}}{\alpha\Gamma(\alpha+1)}\left[-\log(p/\tau)\right]^{\alpha}(1-p/\tau)^{\theta} & \beta=0\\ \dfrac{\overline{Q}\beta^{\alpha+1}}{B(\alpha+1,\beta^{-1})}\left[\left\{1-(p/\tau)^{\beta}\right\}/\beta\right]^{\alpha}(1-p/\tau)^{\theta} & \beta>0\end{cases} \tag{26}$$

Where, $\overline{Q}$ represents the annual mean flow; p denotes the exceeding percentage; τ is the ratio of the number of non-zero flow days to the total number of days. α, β and θ are scaling parameters associated with the physiographic factors and rainfall pattern, which are used to control the shape of FDC. Domains and meanings of these notations are listed in Table 1. It needs to be noticed that the upper bound of β is a variable restricted by the mathematical structure of Beta function. Nash-Sutcliffe Coefficient of Efficiency (*NSCE*) is employed here to measure the distance between observations and model outputs.

$$NSCE=1-\frac{\sum_{i=1}^{n}(Obs_i-Sim_i)^2}{\sum_{i=1}^{n}(Obs_i-\overline{Obs})^2} \tag{27}$$

Where, Obs_i and Sim_i are respectively the *ith* observation and model outputs ranked in descending order, $\overline{Obs}$ is the mean of observations, and n is the length of discharge series.

4. Results and discussions

4.1 Preparation for uncertainty analysis of FDC

In this work, the MCMC sampler derives 10 parallel markov chains, each with a random starting point and a population of 5000 samples. The first 500 of the 5000 samples is used for a burn-in period before the convergence of markov chain to target distribution. For a comparison, GLUE is employed to conduct uncertainty analysis of FDC modeling. GLUE sampler independently runs for 10 times, each time for 10000 samples. *NSCE* is selected as the likelihood function.

4.2 Posterior characteristics for parameter of FDC model

4.2.1 Posterior probability of parameter α

Figure 2 graphically presents the posterior characteristics of parameter α generated respectively by GLUE and MCMC method at different labels (CT=0.1, 0.5, 0.9 for GLUE and *CLM*=0.1, 0.5, 0.9 for MCMC). The best model efficiency of FDC (i.e. *NSCE*) is 0.982 and the corresponding value of parameter α is 0.65, which is calibrated by a SCE-UA approach (Duan et al., 1993). The parameter space around 0.65 is therefore characterized by a high probability. Figure 2(a) and (d) are posterior probability distributions of parameter α by GLUE and MCMC, respectively. The two approaches at low CT or *CLM* always perform poorly in finding the parameter space of high probability (i.e. the parameter space around 0.65), while high labels effectively improve the performance of both approaches. There are differences between MCMC results and GLUE results. Cumulative probability distributions of α by MCMC at all *CLM* follow normal or gamma distribution (Figure 2(e)) whereas those by GLUE do not (Figure 2(b)). The scatters by MCMC are densely concentrated near the high *NSCE* section (Figure 2(f), whereas the scatters by GLUE distribute dispersedly over the whole space (Figure 2(c)). The differences could attribute to the strategies of these two approaches in selection of sampling algorithms and likelihood functions.

Additionally, *CLM* of MCMC can be a value larger than the best *NSCE* (0.982), whereas CT of GLUE cannot. *CLM*=0.99, 0.997 and 0.999 are chosen as examples (Figure 3), the second one of which is a special case where $\sigma_t = \sigma_{obs}$. The posterior density shapes like gamma distribution with slight skewness at all *CLM*, and steepens hugely with the increase of *CLM*. The exploring parameter space narrows sharply in terms of that it changes from [0,1] (*CLM*=0.99) to [0.5,0.8] (*CLM*=0.999).

4.2.2 Posterior probability of other parameters

Posterior distributions of the remaining three model parameters (shown as bar charts, y-axis denotes probability and x-axis parameters values), and the parameters values versus *NSCE* (shown as scatters, y-axis denotes *NSCE* and x-axis parameters values) are presented in Figure 4. Parameter β follows exponential distribution, Q obeys gamma distribution and θ distributes uniformly. However, the features of distributions are changed when *CLM* approaches to 1 (*CLM*=0.997). The distribution of parameter β at *CLM*=0.997 becomes gamma type, and θ follows an exponential distribution. When *CLM*=0.997, the scatters show peaks at the high *NSCE* sections and the ranges of *NSCE* are overly shrunk, indicating that the MCMC search is restricted into a small parameter space.

In short, the approaching of *CLM* to 1 can amplify the microcosmic posterior characteristics of the parameter space with high probability at the cost of abandoning the macroscopical search of remaining parameter space. It could explain why the simulated posterior distributions reported before are always concentrated within very small ranges and why MCMC sampling is often trapped into local maximums (Marshall et al., 2004; Ajami et al., 2007; Kuczera et al., 2007; Blasone et al., 2008b; Vrgut et al., 2009). There are no standards for identifying the best value of *CLM*. The selection of *CLM* could be regarded as a dynamical trade-off between macroscopic versus microcosmic requirements. *CLM* should be selected and adjusted carefully based on practical requirements.

4.2.3 Posterior distributions of correlated parameters and *NSCE*

The correlation between parameter α and β generated by MCMC at different *CLM* are presented in Figure 5. Rapid shrink of exploring parameter space and increase of maximum posterior probability is clearly observed with *CLM* approaching to 1. Samples are clustered in the case of *CLM*=0.999. On the contrary, the probability bars at *CLM*=0.9 cover the whole parameter space, leading to flat distributions, low maximum probabilities and even the occurrence of local maximum probabilities. It tends to be more obvious if *CLM* is settled to a smaller value.

The *NSCE* of FDC derived by MCMC sampler are shown in Figure 6. To the best of our knowledge, it has never been discussed previously. As Figure 6 indicates, the Natural logarithm of the posterior probability densities for *NSCE* approximately accord with a first order linear equation at all *CLM*. It is worth noting that the coefficients of *x* are approximately equivalent to $5.4/(1-CLM)$ and the intercepts at the vertical axis approximately equal to $-In[\sqrt{\pi(1-CLM)}/1.64]-5.4/(1-CLM)$. The results over another 5 basins of north China support the relation as well (Figure S1). The findings above are the powerful evidence to support Eq.20 and the subsequent inferences based on Eq.20. The markov chain tends to convergence if the Natural logarithm of *NSCE* is first-order linearly distributed, which actually provides a simple way to test the convergence to the target distribution. On the other hand, an increasing *CLM* does harm to convergence. The *NSCE* values at the very tails of both sides could not be sufficiently searched with their statistical probability. It may attribute to the difference between real systems and the FDC modeling, as well as the shortcomings of MCMC algorithm. With an increase of *CLM*, the largest posterior probability moves to the largest *NSCE* (0.982) at a cost that the density is biased from the first-order linear distribution. Hence, it is learned that the selection of *CLM* is a trade-off between accurate locating of maximum probability versus convergence to original target distribution.

4.2.4 The effect of data length of observed daily discharge on σ_{obs}

As mentioned above, the algorithmic parameter σ_t is expressed as the product of data length ($\sqrt{n-1}$) and two standard deviations (σ_{Obs} and σ_s). σ_{Obs} is estimated according to the observed data. Therefore, it seems that the data length of observed daily discharge is related to the estimation of σ_{Obs} and then the estimation of σ_t.

In this section, the effect of data length of observed daily discharge on σ_{obs} is investigated. A comparison using different length of data was conducted (Figure 7). The values of σ_{obs} are estimated based on 50%, 70%, 80%, and 90% length of observed discharge data, respectively. The data was randomly sampled from the whole dataset for 1000 times. The 1000 values of σ_{obs} for each dataset (i.e. the different length of discharge data) are aggregated as box plots (Figure 7). The box-plots in Figure 7(a), (b), and (c) show the σ_{obs} values when CLM equals 0.9, 0.99, and 0.997, respectively. The values vary largely for each sampling. The range of values tends to shrink as the data length grows. That is to say, the value of σ_{obs} is more stable when using more data. Besides, the median values of σ_{obs} are almost the same despite of data length, indicating that a stable value of σ_{obs} could be estimated via sampling even though the discharge data is not enough. 1000 times sampling is recommended and the median of σ_{obs} should be employed. Therefore, it could be concluded that different length of data leads to varied values of σ_{obs}, which however is a more stable value through large amount of sampling. Increasing data length gains the stability of estimation of σ_{obs}.

4.3 Posterior characteristics of discharge by GLUE and MCMC methods

4.3.1 Posterior probability density of discharges

To illustrate the posterior characteristics of discharges, three discharge points are selected as examples, namely the 100th, 600th and 1300th discharges in descending order (Figure 8). It is a five-year FDC (1825 days with 237 zero-discharge days), 100th, 600th and 1300th discharges thus could be regarded as the representatives of high, middle and low discharge schemes, respectively. All the posterior densities follow the type of gamma distributions (Figure 8). The posterior density steepens and narrows hugely with the increase of *CLM* (from 0.9 to 0.997). It needs to be pointed out that the algorithmic parameters (r, λ) of the Gamma distributions are calculated based on statistical meaning $\lambda = E(x)/D(x)$ and $r = \lambda E(x)$ rather than through fitting. It indicates that the sampling is statistically reasonable.

The skewness and kurtosis are plotted over the whole probability section in Figure 9. Skewness and kurtosis close to 0 indicates better agreement of the density distribution with normal distribution. Compared with normal distribution, positive kurtosis implies steeper shape, and positive skewness implies a right movement of the maximum probability. The density distribution of discharges at *CLM*=0.9 is steeper and positively biased compared to normal distribution, which is more remarkable at the high and low probability tails. On the contrary, the skewness and kurtosis are always staying at small values throughout the probability section at large *CLM* (*CLM*>0.99), indicating a high similarity with normal distribution. Actually, a large *CLM* (*CLM*>0.99) is consistent to the common settings for σ in previous studies. This could explain why the simulated discharge are normally distributed (Ajami et al., 2007; Noh et al., 2011; Vrgut et al., 2009; Hu et al., 2013).

4.3.2 Properties of 90% confidence intervals

Another important uncertainty measure for a hydrological simulation is the 90%

confidence interval. The deviation between the posterior means and observations (i.e. residuals) and the 90% confidence intervals for residuals at different *CLM* are shown in Figure 10. It is seen that the residuals are valued around 0, indicating that the posterior means of discharge generally match the actual discharge points. Compared to GLUE method at CT=0.9, MCMC method at *CLM*=0.9 yields much thinner and more symmetrical intervals in the low discharge section (i.e. the section with high probability), whereas slightly larger intervals in the high discharge section (i.e. the section with low probability). The 90% confidence interval by GLUE method is evenly spaced but underestimated, especially in the low discharge section. The increase of *CLM* leads to sharp shrink of the band-width, while does not change the shape of upper and lower bounds. A very large *CLM* (>0.99) leads to less coverage ratio of interval for the observed points. The selection of *CLM* is a trade-off between coverage ratio versus band-width of intervals.

5. Conclusions and suggestions

In MCMC approach for uncertainty analysis of hydrological modeling, residuals between model outputs and observations are commonly assumed to follow Gaussian distribution with zero medium and constant standard deviation σ^2. How to identify and estimate parameter σ^2 is a weak point in previous studies. In this work, the statistical meaning of parameter σ^2 of Gaussian-type posterior probability distribution in MCMC method are systemically investigated. Some statistical interpretation and inferences of the parameter are presented to improve the performance of MCMC approach. A new label *CLM* is developed to guide the estimation of σ^2. The uncertainty of the hydrological simulation by a four-parameter FDC model is assessed by means of MCMC method based on *CLM*, and the GLUE method is employed for comparison.

Uncertainty analysis here is conducted concerning the posterior characteristics of model parameters, discharges and confidence intervals. A series of derivative conclusions are therefore achieved and major findings are summarized as follows.

(1) Parameter σ is statistically related not only to the observation but also to model calibration. σ is expressed as the product of data length ($\sqrt{n-1}$) and two standard deviations, one of which is for observations (i.e. σ_{Obs}) and the other for Nash-Sutcliffe Coefficient of Efficiency (*NSCE*) (i.e. σ_s). A new label called Confidence Level of Model (*CLM*) is developed to interpret σ_s. The natural logarithm of the posterior probability for *NSCE* could be expressed as a first-order linear equation associated with *CLM*, which is practically demonstrated by a series of case studies about the posterior density of *NSCE*.

(2) *CLM* is a label representing the manually-decided minimum of acceptable *NSCE*. *CLM* is more meaningful and dynamic than CT used in GLUE. It is a procedure-oriented label used for shaping the target distribution. It can be set as a probabilistic variable or a constant. Case studies reveal that *CLM* remarkably affects the value of σ and the MCMC results. It is recommended to identify the algorithmic parameter σ according to *CLM*.

(3) Different length of data leads to varied values of σ_{obs}, which however could be a more stable value through large amount of sampling. 1000 times sampling is recommended and the median of σ_{obs} should be employed. Increasing data length gains the stability of estimation of σ_{obs}.

(4) The MCMC method based on *CLM* performs well in generating regular posterior distributions of model parameters and discharges, and in yielding narrow and symmetrical confidence intervals. The estimation of *CLM* is related to three kinds of

trade-offs, including the one between macroscopic versus microcosmic requirements, the one between accurate locating of maximum probability versus convergence to original target distribution, and the one between coverage ratio versus band-width of intervals.

Findings in this paper could well interpret the problems commonly encountered in traditional Bayesian uncertainty assessments and provide insights for uncertainty analysis of other environmental modeling. Nevertheless, strict mathematical proof of Eq.18 as well as the application of *CLM* in more complex models is necessary. It will be further studied in our future work.

Acknowledgments. The work was jointly supported by grants from the National Natural Science Foundation of China (51809072, 51879068), and a grant from the China Postdoctoral Science Foundation (2020M671322).

References:

Ajami, N. K., Duan, Q., & Sorooshian, S. 2007. An integrated hydrologic Bayesian multimodel combination framework: Confronting input, parameter, and model structural uncertainty in hydrologic prediction. Water Resources Research, *43*(1).

Beven, K., & Binley, A. 1992. The future of distributed models: model calibration and uncertainty prediction. Hydrological processes, 6(3), 279-298.

Beven, K., & Freer, J. 2001. Equifinality, data assimilation, and uncertainty estimation in mechanistic modelling of complex environmental systems using the GLUE methodology. Journal of hydrology, 249(1-4), 11-29.

Blasone, R. S., Madsen, H., & Rosbjerg, D. 2008a. Uncertainty assessment of integrated distributed hydrological models using GLUE with Markov chain Monte Carlo sampling. Journal of Hydrology, 353(1-2), 18-32.

Blasone, R. S., Vrugt, J. A., Madsen, H., Rosbjerg, D., Robinson, B. A., & Zyvoloski, G. A. 2008b. Generalized likelihood uncertainty estimation (GLUE) using adaptive Markov Chain Monte Carlo sampling. Advances in Water Resources, 31(4), 630-648.

Bouda, M., Rousseau, A. N., Konan, B., Gagnon, P., & Gumiere, S. J. 2011. Bayesian uncertainty analysis of the distributed hydrological model HYDROTEL. Journal of Hydrologic Engineering, 17(9), 1021-1032.

Choi, H. T., & Beven, K. 2007. Multi-period and multi-criteria model conditioning to reduce prediction uncertainty in an application of TOPMODEL within the GLUE framework. Journal of Hydrology, 332(3-4), 316-336.

Chung, E. S., & Kim, S. U. 2013. Bayesian rainfall frequency analysis with extreme value using the informative prior distribution. KSCE Journal of Civil Engineering, 17(6), 1502-1514.

Cryer, S. A., & Applequist, G. E. 2003. Direct treatment of uncertainty: II—Applications in pesticide runoff, leaching and spray drift exposure modeling. Environmental engineering science, 20(3), 169-181.

Cui, T., Yang, T., Xu, C. Y., Shao, Q., Wang, X., & Li, Z. 2018. Assessment of the impact of climate change on flow regime at multiple temporal scales and potential ecological implications in an alpine river. Stochastic Environmental Research and Risk Assessment, 32(6), 1849-1866.

Duan, Q. Y., Gupta, V. K., & Sorooshian, S., 1993. Shuffled complex evolution approach for effective and efficient global minimization. Journal of optimization theory and applications, 76(3), 501-521.

Engeland, K., & Gottschalk, L. 2002. Bayesian estimation of parameters in a regional hydrological model. Hydrology and Earth System Sciences Discussions, 6(5), 883-898.

Guse, B., Pfannerstill, M., Strauch, M., Reusser, D. E., Lüdtke, S., Volk, M., ... & Fohrer, N. 2016. On characterizing the temporal dominance patterns of model parameters and processes. Hydrological Processes, 30(13), 2255-2270.

Hassan, A. E., Bekhit, H. M., & Chapman, J. B. 2008. Uncertainty assessment of a stochastic groundwater flow model using GLUE analysis. Journal of Hydrology, 362(1-2), 89-109..

Hu, Y. M., Liang, Z. M., Li, B. Q., & Yu, Z. B. 2013. Uncertainty assessment of hydrological frequency analysis using bootstrap method. Mathematical Problems in Engineering, 2013.

Huang, C. S., Yang, T., Yeh, H. D. 2018. Review of analytical models to stream depletion induced by pumping: guide to model selection. Journal of hydrology, 561, 277-285.

Jin, X., Xu, C. Y., Zhang, Q., & Singh, V. P. 2010. Parameter and modeling uncertainty simulated by GLUE and a formal Bayesian method for a conceptual hydrological model. Journal of Hydrology, 383(3-4), 147-155.

Kavetski, D., Kuczera, G., & Franks, S. W. 2006. Bayesian analysis of input uncertainty in hydrological modeling: 2. Application. Water Resources Research, 42(3).

Kuczera, G., & Parent, E. 1998. Monte Carlo assessment of parameter uncertainty in conceptual catchment models: the Metropolis algorithm. Journal of Hydrology, 211(1-4), 69-85.

Kuczera, G., Kavetski, D., Renard, B., & Thyer, M. 2007. Bayesian total error analysis for hydrologic models: Markov Chain Monte Carlo methods to evaluate the posterior distribution. Mod. and Simul. Soc. of Aust. and NZ, Christchurch, NZ.

Kuczera, G., Kavetski, D., Renard, B., & Thyer, M. 2010. A limited- memory acceleration strategy for MCMC sampling in hierarchical Bayesian calibration of hydrological models. Water Resources Research, 46(7).

Kumar, A., Yang, T., & Sharma, M. P. 2019. Long-term prediction of greenhouse gas risk to the Chinese hydropower reservoirs. Science of the Total Environment, 646, 300-308.

Lee, K. S., & Kim, S. U. 2008. Identification of uncertainty in low flow frequency analysis using Bayesian MCMC method. Hydrological Processes, 22(12), 1949-1964.

Liang, F. 2005. Bayesian neural networks for nonlinear time series forecasting. Statistics and Computing, 15(1), 13-29.

Li, Z., Yang, T., Huang, C. S., Xu, C. Y., Shao, Q., Shi, P., ... & Cui, T. 2018a. An improved approach for water quality evaluation: TOPSIS-based informative weighting and ranking (TIWR) approach. Ecological Indicators, 89, 356-364.

Li, X., Babovic, V., 2018b. A new scheme for multivariate, multisite weather generator with inter-variable, inter-site dependence and inter-annual variability based on empirical copula approach, Climate Dynamics, 1-21.

Li, X., Meshgi, A., Wang, X., Zhang, J., Tay, S. H. X., Pijcke, G., ... & Babovic, V. 2018c. Three resampling approaches based on method of fragments for daily-to-subdaily precipitation disaggregation. International Journal of Climatology, 38, e1119-e1138.

Marshall, L., Nott, D., & Sharma, A. 2004. A comparative study of Markov chain Monte Carlo methods for conceptual rainfall-runoff modeling. Water Resources Research, 40(2).

Marshall, L., Nott, D., & Sharma, A. 2005. Hydrological model selection: A Bayesian alternative. Water resources research, 41(10).

Naji, A., Cheng, A. D., & Ouazar, D. 1998. Analytical stochastic solutions of saltwater/freshwater interface in coastal aquifers. Stochastic Hydrology and Hydraulics, 12(6), 413-430.

Noh, S., Tachikawa, Y., Shiiba, M., & Kim, S. 2011. Applying sequential Monte Carlo methods into a distributed hydrologic model: lagged particle filtering approach with regularization. Hydrology and Earth System Sciences,15(10), 3237-3251.

Ouarda, T. B. M. J., & El-Adlouni, S. 2011. Bayesian nonstationary frequency analysis of hydrological variables. JAWRA Journal of the American Water Resources Association, 47(3), 496-505.

Reis, D. S., & Stedinger, J. R. 2005. Bayesian MCMC flood frequency analysis with historical information. *Journal of Hydrology*, *313*(1), 97-116.

Ren, W., Yang, T., Shi, P., Xu, C. Y., Zhang, K., Zhou, X., ... & Ciais, P. 2018. A probabilistic method for streamflow projection and associated uncertainty analysis in a data sparse alpine region. Global and Planetary Change, 165, 100-113.

Rosenblueth, E. 1975. Point estimates for probability moments. Proceedings of the National Academy of Sciences, 72(10), 3812-3814.

Shao, Q., Zhang, L., Chen, Y. D., & Singh, V. P. 2009. A new method for modelling flow duration curves and predicting streamflow regimes under altered land-use conditions. Hydrological Sciences Journal, 54(3), 606-622.

Shi, P., Yang, T., Xu, C. Y., Yong, B., Shao, Q., Li, Z., ... & Li, S. 2017. How do the multiple large-scale climate oscillations trigger extreme precipitation?. Global and Planetary Change, 157, 48-58.

Thiemann, M., Trosset, M., Gupta, H., & Sorooshian, S. 2001. Bayesian recursive parameter estimation for hydrologic models. Water Resources Research, 37(10),

2521-2535.
Thyer, M., Kuczera, G., & Wang, Q. J. 2002. Quantifying parameter uncertainty in stochastic models using the Box-Cox transformation. Journal of Hydrology, 265(1), 246-257.
Vrugt, J. A., Gupta, H. V., Bastidas, L. A., Bouten, W., & Sorooshian, S. 2003a. Effective and efficient algorithm for multiobjective optimization of hydrologic models. Water Resources Research, 39(8).
Vrugt, J. A., Gupta, H. V., Bouten, W., & Sorooshian, S. 2003b. A Shuffled Complex Evolution Metropolis algorithm for optimization and uncertainty assessment of hydrologic model parameters. Water Resources Research,39(8).
Vrugt, J. A., Ter Braak, C. J., Gupta, H. V., & Robinson, B. A. 2009. Equifinality of formal (DREAM) and informal (GLUE) Bayesian approaches in hydrologic modeling?. Stochastic environmental research and risk assessment, 23(7), 1011-1026.
Wang, X., Yang, T., Wortmann, M., Shi, P., Hattermann, F., Lobanova, A., & Aich, V. 2017. Analysis of multi-dimensional hydrological alterations under climate change for four major river basins in different climate zones. Climatic change, 141(3), 483-498.
Wang, X., Yang, T., Yong, B., Krysanova, V., Shi, P., Li, Z., & Zhou, X. 2018. Impacts of climate change on flow regime and sequential threats to riverine ecosystem in the source region of the Yellow River. Environmental Earth Sciences, 77(12), 465.
Yang, J., Reichert, P., & Abbaspour, K. C. 2007. Bayesian uncertainty analysis in distributed hydrologic modeling: A case study in the Thur River basin (Switzerland). Water resources research, 43(10).
Yang, T., Cui, T., Xu, C. Y., Ciais, P., & Shi, P. 2017. Development of a new IHA method

for impact assessment of climate change on flow regime. Global and Planetary Change, 156, 68-79.

Zhang, X., Liang, F., Srinivasan, R., & Van Liew, M. 2009. Estimating uncertainty of streamflow simulation using Bayesian neural networks. Water resources research, 45(2).

Figure

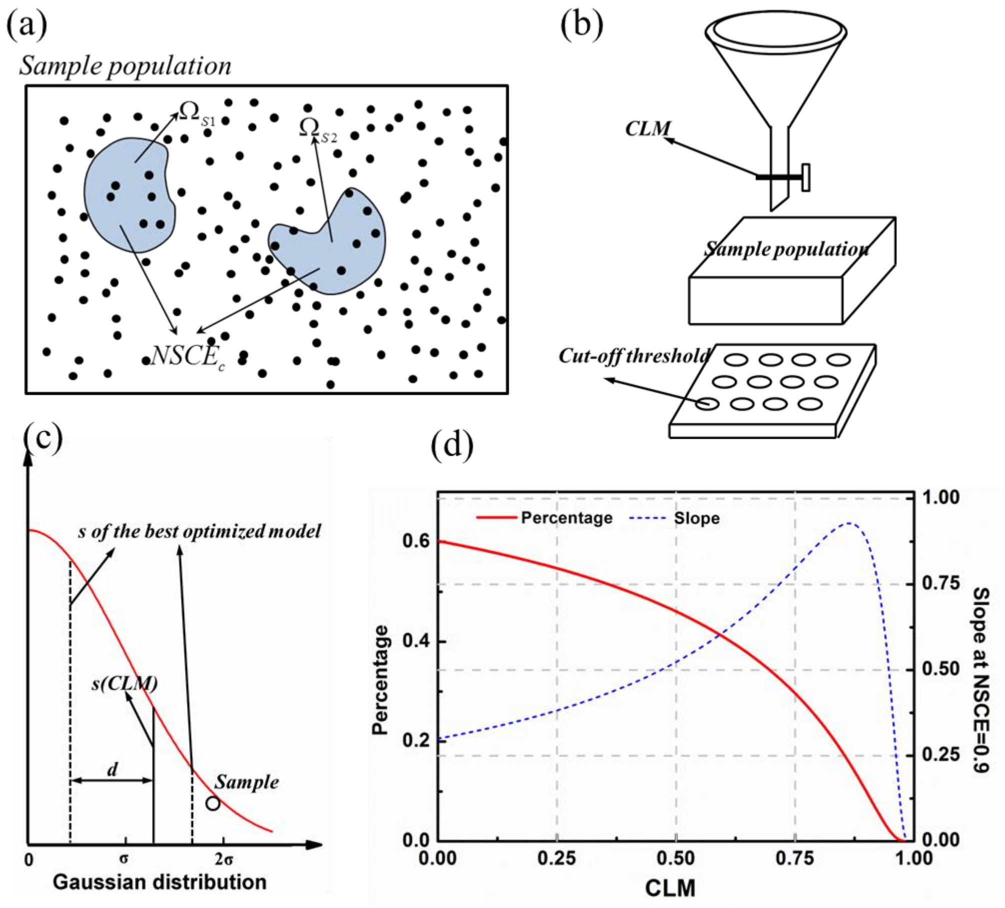

Figure 1. Sample population of MCMC approach (a); Schematic map for the function of CLM and cut-off threshold (b); Distribution of variable *s* (the right half of common normal distribution) (c); The percentage of the actual sampling space to the originally assumed sampling space and the slope of the probability density at NSCE=0.9 versus the CLM (d).

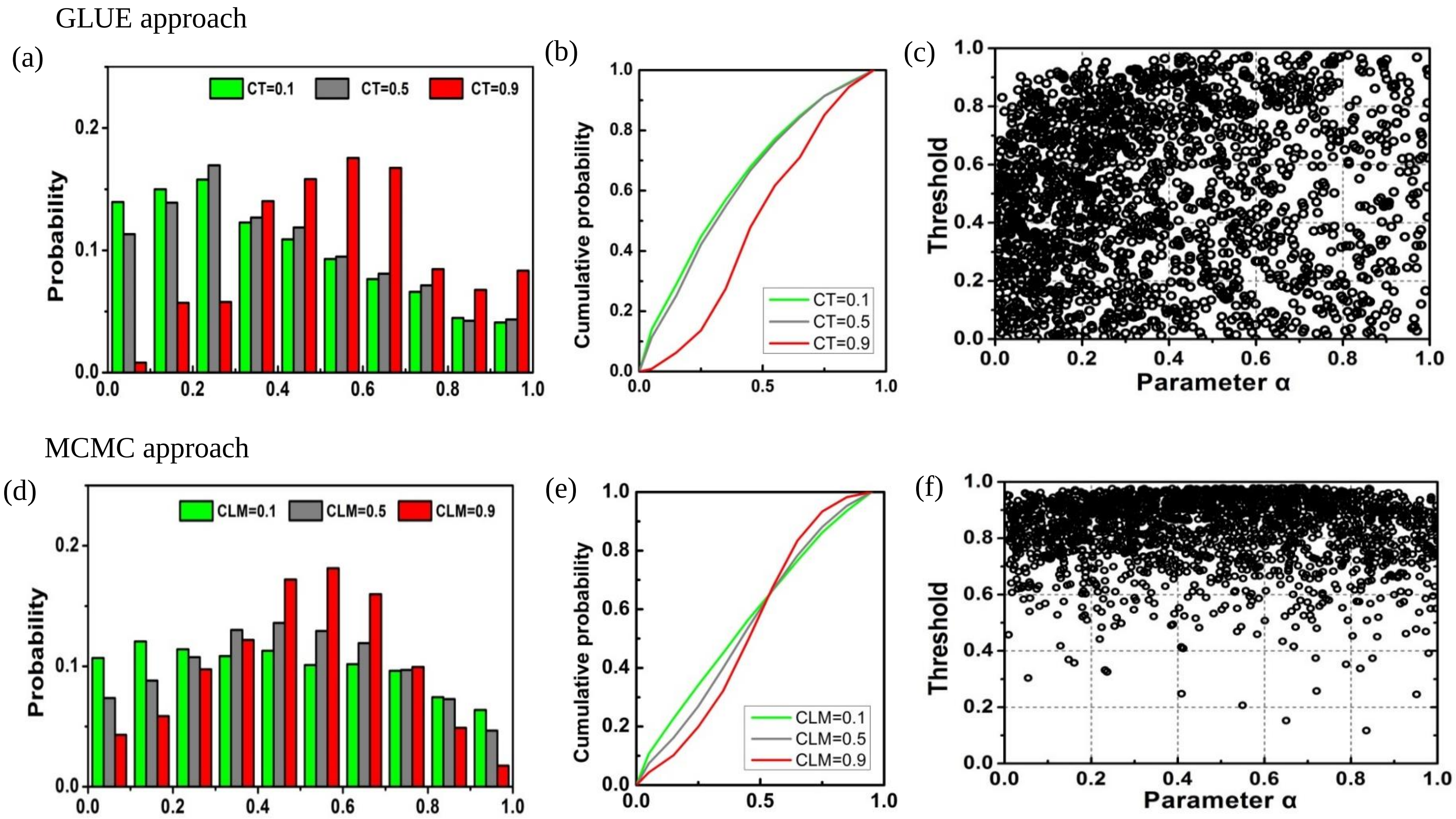

Figure 2. Posterior probability (a); Cumulative probability of parameter α by GLUE method at the cut-off threshold=0.1, 0.5 and 0.9 (b); Scatters of parameter α by GLUE method versus thresholds (c); Posterior probability (d); Cumulative probability of parameter α by MCMC method at CLM=0.1, 0.5 and 0.9 (e); Scatters of parameter α generated by MCMC method versus thresholds at CLM=0.5 (f).

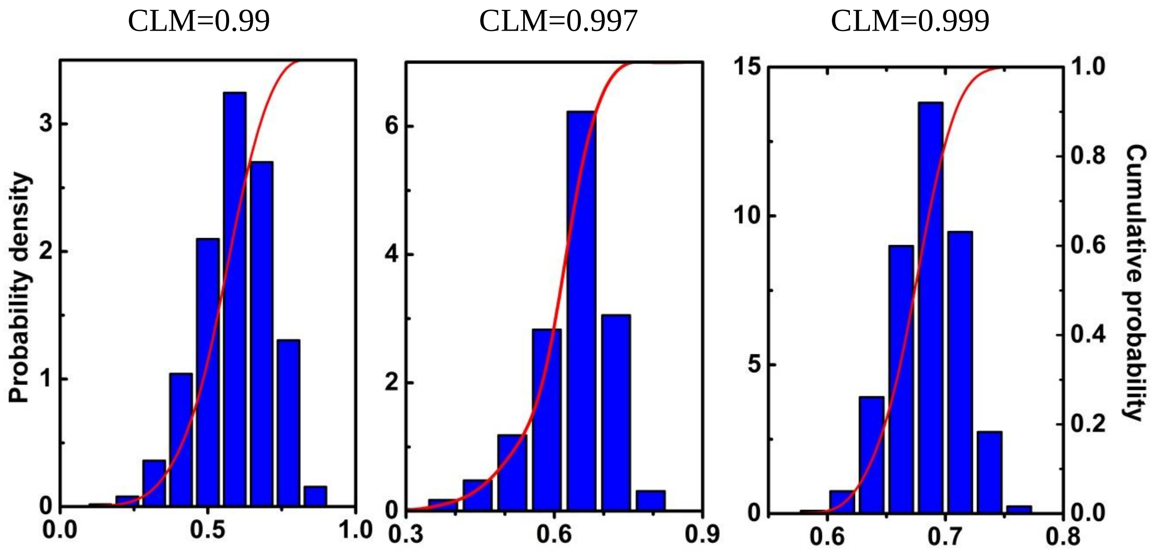

Figure 3. Posterior probability density and cumulative probability generated by MCMC approach at CLM=0.99, 0.997 and 0.999, respectively.

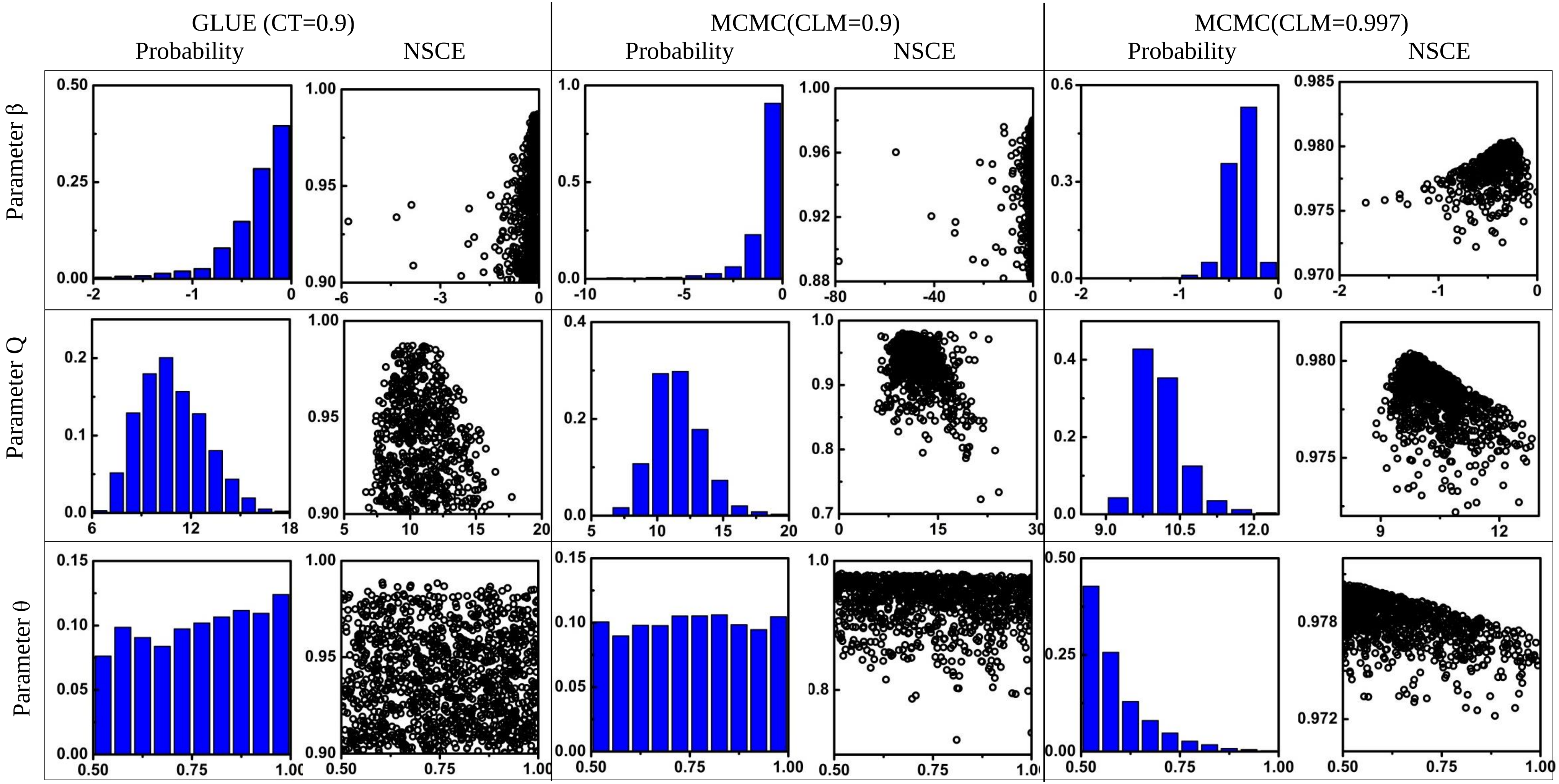

Figure 4. Posterior probability distributions for parameter β, Q and θ, and their scatters against thresholds

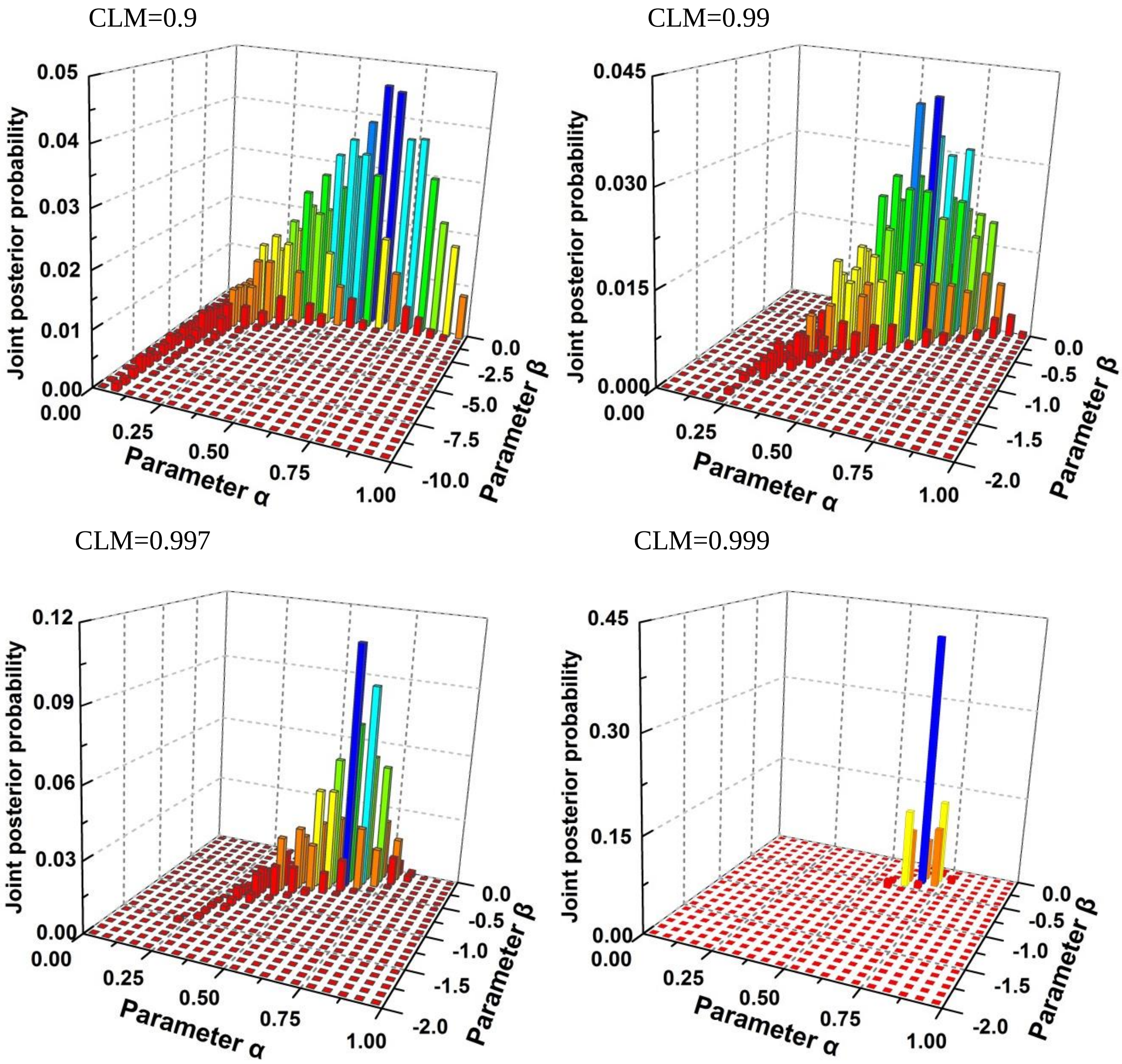

Figure 5. Bars of the joint posterior probability distribution for parameter α and β generated by MCMC approach at different CLMs (CLM=0.9, 0.99, 0.997 and 0.999)

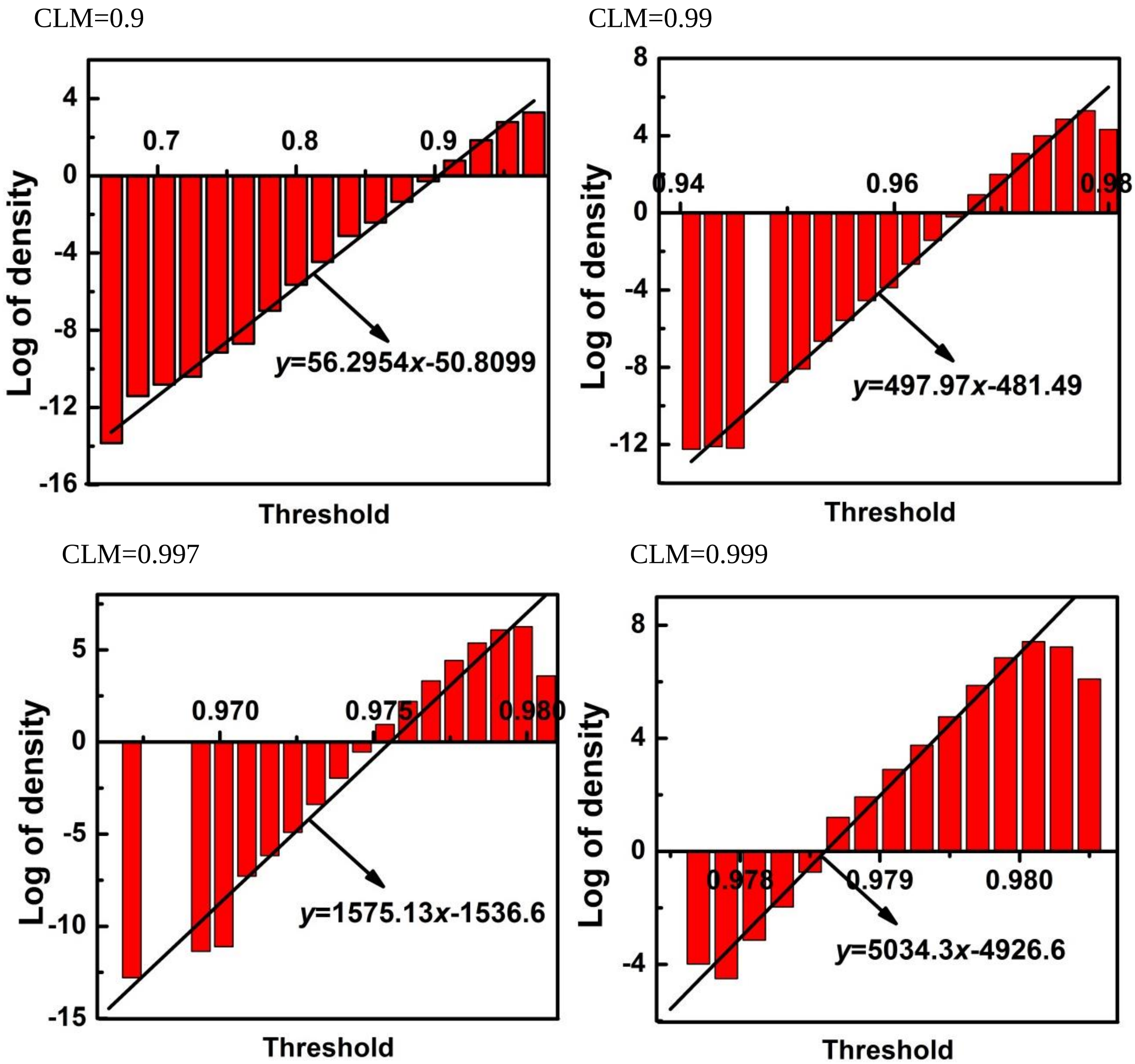

Figure. 6 Natural logarithm of the posterior probability densities generated by MCMC approach at different CLMs (CLM=0.9, 0.99, 0.997 and 0.999) against the NSCEs

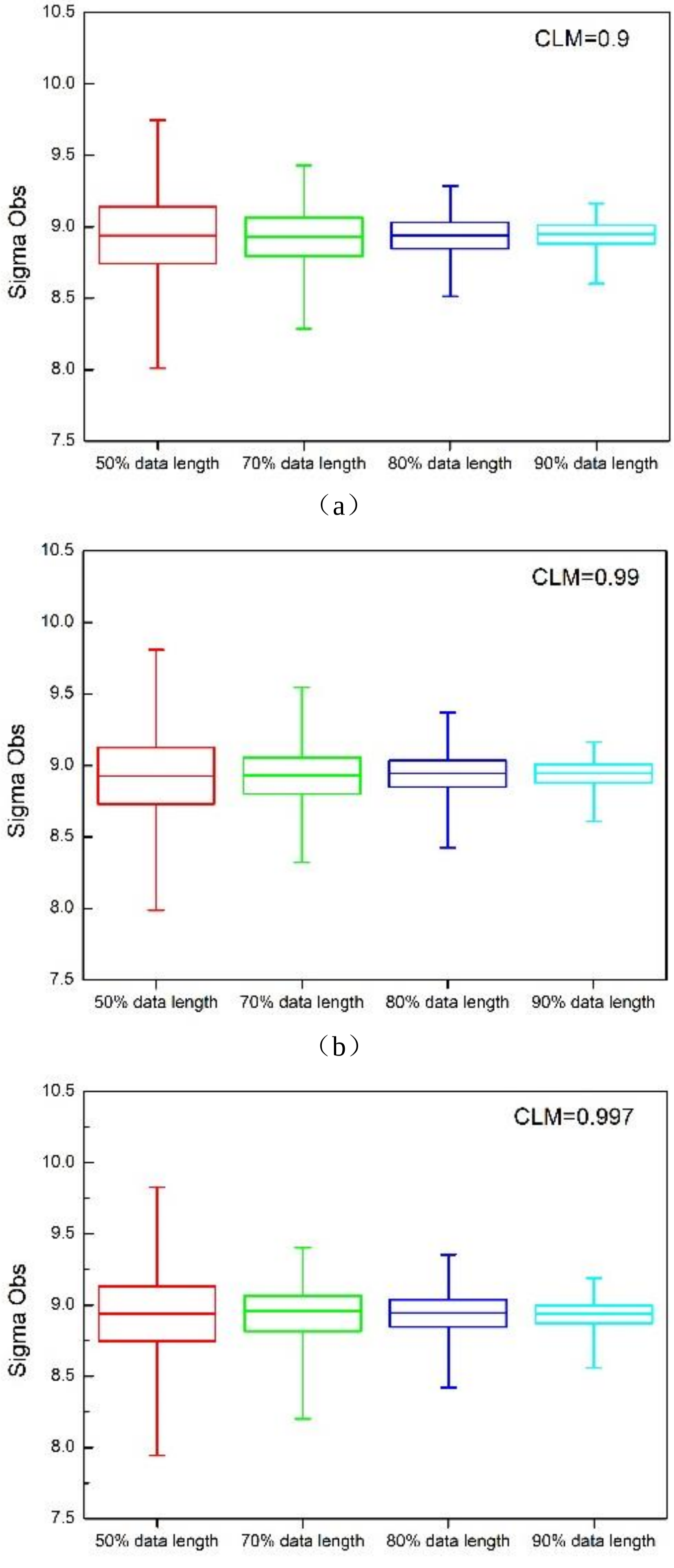

Figure. 7 The values of σ_{Obs} based on different data length of observed daily discharge when CLM=0.9, 0.99, and 0.997, respectively.

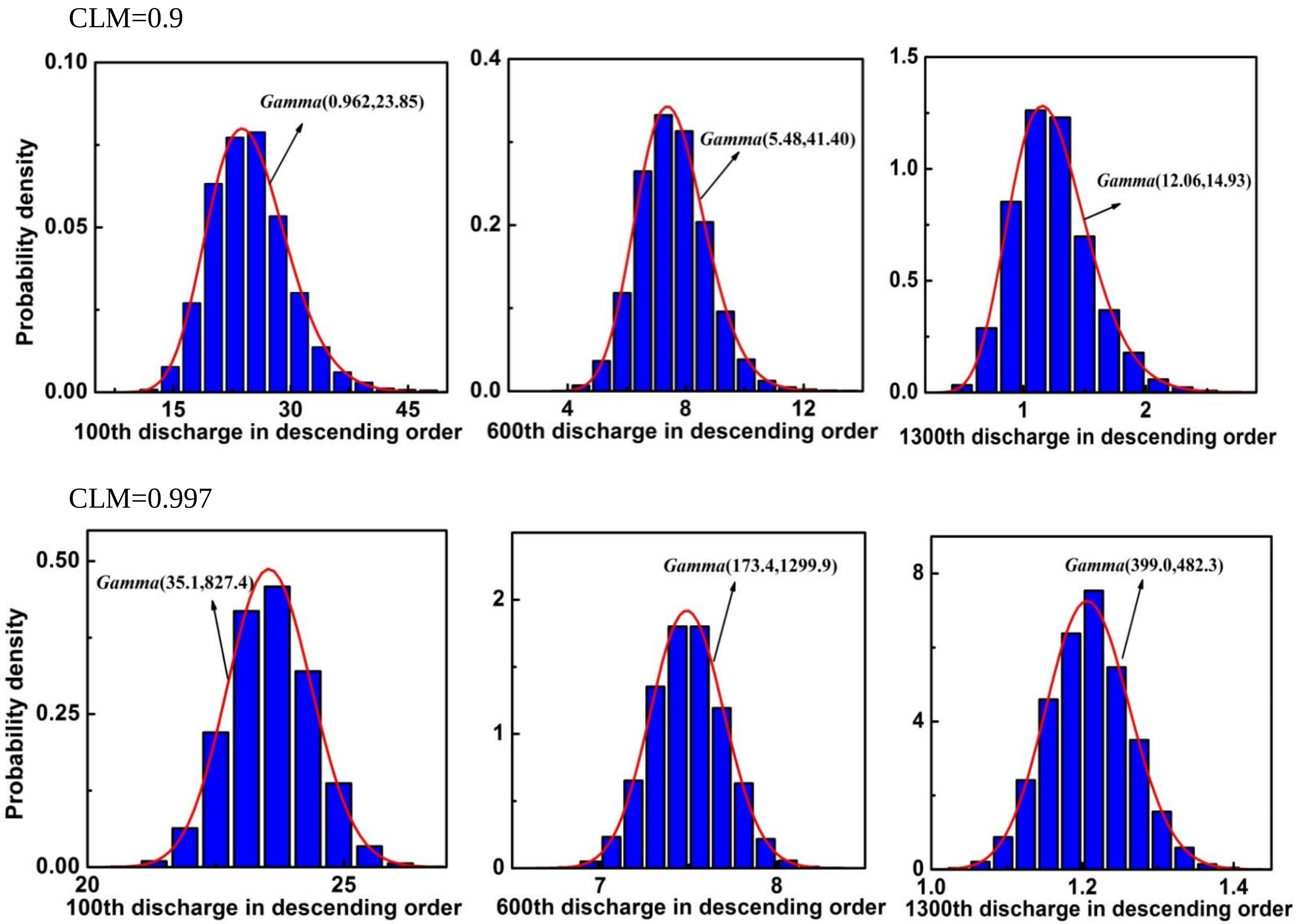

Figrue 8. Posterior probability density for the 100th, 600th and 1300th discharges in descending order by MCMC approach at CLM=0.9 and 0.997

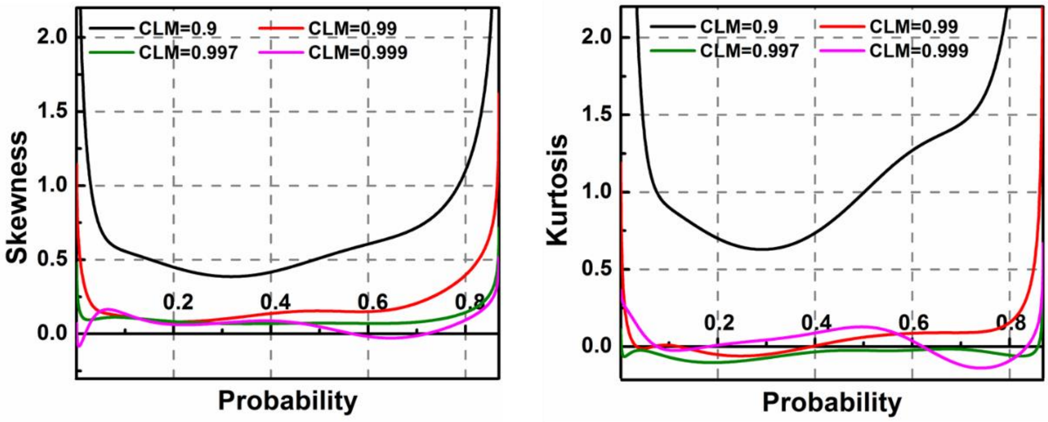

Figure 9. Skewness and kurtosis of posterior probability densities for discharge over the whole probabilty domain by MCMC approach at CLM=0.9, 0.99, 0.997 and 0.999

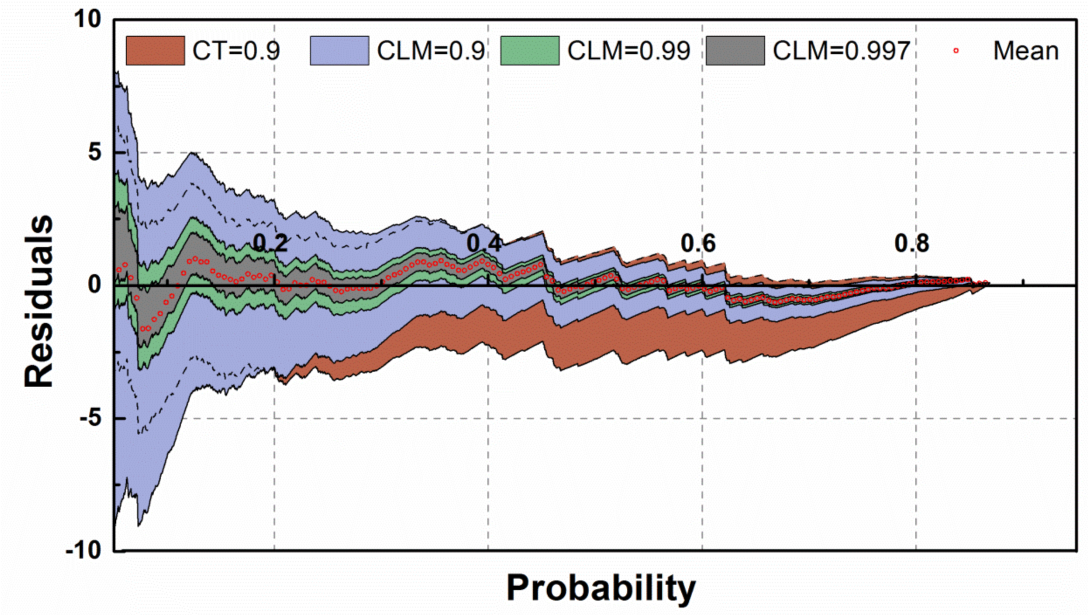

Figure 10. The residuals and the 90% confidence intervals for residuals at different CLMs (CLM=0.9, 0.99, 0.997 and 0.999) and CT=0.9.

Table 1. Descriptions and domains of notations involved in the FDC model

Parameter	Description	Units	Domain
α	shape parameter impacted by rainfall patterns and physiographic factors	[-]	[0,1.0]
β	shape parameter impacted by rainfall patterns and physiographic factors	[-]	[-100,100]
Q	annual mean flow	[m^3/s]	[0,50]
θ	shape parameter impacted by rainfall patterns and physiographic factors	[-]	[0.5,1.0]
$\alpha \cdot \beta$	constricted by Beta function	[-]	[-1,0]

CRediT authorship contribution statement

Pengfei Shi: Conceptualization, Formal analysis, Investigation, Methodology, Resources, Validation, Visualization, Writing - original draft, Funding acquisition, Writing - review & editing. **Tao Yang:** Conceptualization, Formal analysis, Investigation, Resources, Visualization, Writing - original draft, Funding acquisition. **Bin Yong:** Data curation, Formal analysis, Methodology, Software, Writing - original draft. **Chong-Yu Xu:** Conceptualization, Methodology, Resources, Supervision, Validation, Visualization, Writing-review & editing. **Zhenya Li:** Data curation, Formal analysis, Investigation, Methodology, Writing - review & editing. **Xiaoyan Wang:** Formal analysis, Methodology, Resources, Validation. **Youwei Qin:** Formal analysis, Methodology, Resources, Validation. **Xudong Zhou**: Formal analysis, Methodology, Resources, Validation.